A frequency-time domain method for annual energy production estimation in floating wind turbines

A frequency-time domain method for annual energy production estimation in floating wind turbines

R Amaral[1], K Laugesen[2], M Masciola[3], D von Terzi[4], P Deglaire[5] and A Viré[6]

[1] Technische Universiteit Delft (TU Delft), Kluyverweg 1, 2629 HS Delft, Netherlands
[2] Siemens Gamesa Renewable Energy (SGRE), Borupvej 16, 7330 Brande, Denmark
[3] Siemens Gamesa Renewable Energy (SGRE), 1050 Walnut Suite 303 Boulder Colorado 80302, United States
[4] Technische Universiteit Delft (TU Delft), Kluyverweg 1, 2629 HS Delft, Netherlands
[5] Siemens Gamesa Renewable Energy (SGRE), Avenue de l'Université C/O Insa Rouen - BP 08, 76800 Saint Étienne de Rouvray, France
[6] Technische Universiteit Delft (TU Delft), Kluyverweg 1, 2629 HS Delft, Netherlands

E-mail: r.p.elisbaomartinsamaral@tudelft.nl

Abstract. A new method is proposed to estimate a floating wind turbine's annual energy production (AEP) using frequency and time-domain design techniques. The approach demonstrated herein estimates the AEP by performing a convolution between the floating platform response and the response power operators (RPOs) that map the average power produced by the turbine as a function of the amplitude and frequency of the platform motions. One advantage of this approach is that it can be performed early in the conceptual design phase to help discover design space trade-offs between the platform and rotor design. The methodology is applied to the IEA Wind 15 MW WindCrete spar-buoy model using OpenFAST. The RPOs are obtained by prescribing single-DOF platform motions to the turbine with a given amplitude and frequency. This methodology is then validated by comparing the AEP estimation from the RPOs with the AEP estimation from fully-coupled simulations. The results indicate that the method is able to estimate the value of AEP for a realistic sea-state and regular waves. However, further validation is needed as, in the first case, the turbine is moving too little and, in the second case, the contribution of the controller may be dominant.

1. Introduction

Nowadays, in the floating offshore wind turbine (FOWT) industry, the design of the floating platform and the wind turbine is performed in a decoupled way to a great extent. The result is that both the wind turbine and floater designers often exchange low-fidelity models early on in the concept-inception stage and then steadily increase fidelity as the design space narrows to achieve an optimal configuration. Optimizing the floater for annual energy production (AEP) requires running thousands of aero-elasto-servo-hydrodynamic coupled simulations - or simply fully-coupled simulations - per optimization loop. Besides this, multiple loops may be necessary before a satisfactory floater design is achieved, and multiple floaters may be considered in a given project. Facing such a massive number of simulations, it is of interest to have a preliminary design process that makes it possible to understand how frequency-domain decisions related to the floater affect AEP while using fewer and faster simulations.

2. Objectives

This paper describes a proof-of-concept study of a frequency-time domain preliminary design method that attempts to meet the needs mentioned before by replacing the traditional fully-coupled simulations with simulations where the motion of the turbine is prescribed. These are designated as prescribed motion simulations. Validation is done by benchmarking the AEP estimated using the proposed method for specific sea-states against fully-coupled simulations. As such, this paper lays down the foundation for the development of what could potentially become a more time-efficient and complete tool for AEP estimation.

3. Methodology

The new method is used to estimate the AEP of a FOWT when subjected to a given sea-state spectrum. Instead of a full physics coupling, the hydrodynamics is decoupled from the rest of the physics in the considered simulations. The hydrodynamic solver is not active, and hence there are no hydrodynamic loads driving the motion. Rather than this, the motion is prescribed by the user to assess the power production characteristics. A single oscillation frequency and amplitude are prescribed per simulation to emulate the FOWT motion in monochromatic waves. Figure 1 shows the method in detail, where three distinct parts, P1, P2 and P3, can be identified.

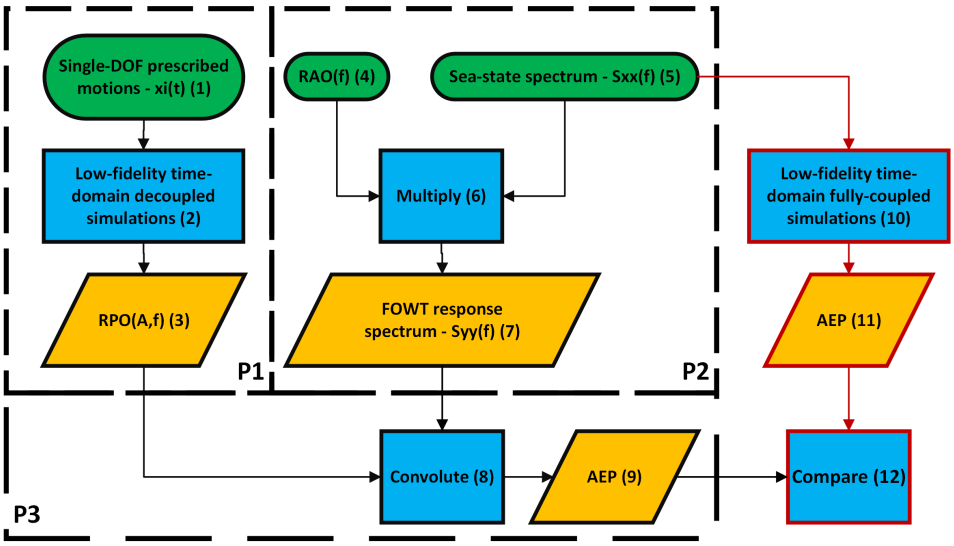

Figure 1: AEP estimation method and validation procedure. Green, blue and yellow figures represent starting inputs, processes and input/output data, respectively. The black and red arrows and boxes indicate the method itself and the validation path, respectively. "P" stands for "Part". "RPO" stands for "Response Power Operators". "A" and "f" stand for "Amplitude" and "frequency", respectively. "RAO" stands for "Response Amplitude Operators". "Low-fidelity" refers to time-domain methods based on the blade element momentum theory (BEMT).

In P1, many simulations (2) with prescribed turbine motion (1) are performed. In each of the simulations, only one platform degree-of-freedom (DOF) out of six is enabled and its motion is described by a sinusoid with a set amplitude A and frequency f. These two parameters should be considered in realistic operating ranges to limit computational expense. The remaining platform DOFs are disabled and retain the value equal to the initial condition throughout the simulation. These initial conditions should be set according to the average value that the specific DOF is

expected to take under the considered operating conditions. This requires some prior knowledge or preliminary calculations. Taking pitch, for example, one can use the wind speed to estimate the thrust and use it in a force balance to estimate the platform pitch angle. The objective of P1 is to produce the response power operators (RPOs) (3) that map the average power as a function of the amplitude and frequency of the prescribed motion in each DOF. In P2, the RAOs (4) are assumed to be an input from the floater designer. This block is updated with every new floater design to compute the AEP change between designs. The RAOs are used to estimate the response spectrum of the turbine motion S_{yy} (7) when subjected to a given sea-state spectrum S_{xx} (5) through simple multiplication in the frequency domain (6), which corresponds to a convolution in the time domain. Finally, in P3, the RPOs (3) and the response spectrum S_{yy} (7) are convoluted in a suitable way (8), yielding the AEP estimate of the turbine (9) for the considered sea-state spectrum. To validate the approach (12), this value is then compared against the AEP (11) obtained from fully-coupled simulations (10) where the turbine is subjected to the same aerodynamic conditions as in (2) and sea-state as in (5). No second-order waves nor second-order platform loads were enabled. This method was applied to the WindCrete spar-buoy model developed in the EU-funded COREWIND project [1] using OpenFAST 2.4 [2]. The original model had been made for OpenFAST 2.1, so some input variables had to be added/removed from the input files. The Linux compatible dynamic library necessary to run the controller was not functional, so the one available in [3] was used instead. The different parts of the method, P1, P2 and P3, are further detailed in the following sections.

4. Response power operators - RPO(A,f)

In OpenFAST 2.4 [2], the platform's motion cannot be directly prescribed. This problem was bypassed through the use of the ExtPtfm module [4] that models the foundation as a super-element with a given mass m_{ij}, damping c_{ij} and stiffness k_{ij} tensors. Force time-histories $F_i(t)$ were then applied to it in order to obtain the desired motion. In order to have the dynamics entirely driven by the super-element and the forces prescribed to it, it is essential to make m_{ij} much larger than the original mass tensor of the turbine. This was achieved by multiplying each of the original masses and inertias by a tunable order of magnitude (see equation (1)). c_{ij} and k_{ij} were related to m_{ij} by relations used in the Seismic Module of FAST v7 [5], where the force prescription method was also used (see equations (2)-(4)).

$$m_{ij} = \begin{bmatrix} 10^{p_1} m_{Surge} & 0 & 0 & 0 & 0 & 0 \\ 0 & 10^{p_2} m_{Sway} & 0 & 0 & 0 & 0 \\ 0 & 0 & 10^{p_3} m_{Heave} & 0 & 0 & 0 \\ 0 & 0 & 0 & 10^{p_4} I_{Roll} & 0 & 0 \\ 0 & 0 & 0 & 0 & 10^{p_5} I_{Pitch} & 0 \\ 0 & 0 & 0 & 0 & 0 & 10^{p_6} I_{Yaw} \end{bmatrix} \quad (1)$$

$$k_{ij} = \omega^2 m_{ij} \quad (2) \qquad c_{ij} = 2\omega m_{ij}\zeta \quad (3) \qquad \zeta = \frac{c_{ij}}{c_{ij_{crit.}}} = 0.65 \quad (4)$$

m_{ij} is a diagonal mass tensor whose components correspond to the prescribed mass or inertia in the six DOFs (the same is said for c_{ij} with respect to damping and for k_{ij} with respect to stiffness); p_i with $i = \{1, 2, 3, 4, 5, 6\}$ are tunable exponents; m_{DOF} and I_{DOF} with $DOF = \{Surge, Sway, Heave, Roll, Pitch, Yaw\}$ are the original masses/inertias of the turbine; $\omega = 2\pi f$ and f are the prescribed motion angular frequency and frequency, respectively; $c_{ij_{crit.}}$ is the critical damping and $\zeta = 0.65$ is the damping ratio which is an arbitrary constant in the recommended interval of [0.6;0.7] [5].

The tensors are diagonal so that the DOFs are decoupled and controlled independently. The

force time-histories were obtained from the tensors and the desired prescribed motion according to the linear system response to constant and periodic excitations of constant amplitude [6]:

$$F_i(t) = \begin{cases} k_{ij} \cdot x_j(t), & \text{if } x_j(t) = C \\ \sqrt{(k_{ij} - m_{ij}\omega^2)^2 + (c_{ij}\omega)^2} \cdot x_j(t), & \text{if } x_j(t) = Asin(\omega t) \end{cases} \quad (5)$$

$x_j(t)$ is the desired prescribed motion time-history; A is the amplitude; C is a constant.

There is a phase difference between F_i and the obtained motion but it is irrelevant as it is a simple shift in time. By contrast, it is crucial to obtain the correct amplitude A and frequency f. All the prescribed motions were verified. A visual scan was first performed to check the general shape of the sinusoids and identify severe errors. Afterward, a more analytical approach was taken. The average amplitude of each simulation was calculated as half of the difference between the average maxima and the average minima of the displacement. The average frequency was calculated as half of the average of the inverses of the time intervals between consecutive maxima and minima. Not very often, the sinusoids had extremes in unexpected locations because they were locally not perfect as the result of other forces arising from the turbine. As a consequence, only extremes within a 10% tolerance from the expected value of amplitude and frequency were considered. The average values of the amplitude and frequency were then compared to the prescribed ones using sequentially lower tolerances to estimate the maximum error. The surge and heave simulations had an error lower than 3% of the prescribed amplitude for every simulation. All but two of the pitch simulations had an error lower than 3%. The exceptions were sporadic and demonstrated unusual amplitudes in one of the oscillations after the transient. Similar situations had been encountered for roll and running those simulations with a fixed rotor speed and the controller turned off made the amplitude bumps go away. The problem was thus attributed to the controller. The average amplitude was nevertheless very close to the prescribed amplitude and the simulations were included in the results.

The RPOs are the amplitude-frequency response function of the average power of the turbine. The aerodynamic power was used instead of the generator power to reduce the number of factors influencing the results. Still, this methodology is fully compatible with using the generator power. The average power was calculated for each simulation by taking the average of the aerodynamic power time series after a certain transient period. Previous studies for simulations with turbulence showed that 400 s were enough, so this value was used. There is nonetheless room for optimization since no turbulence was considered. The number of periods necessary to achieve the average power convergence after the transient period was determined by performing 50-period simulations and then extracting the number of periods after which the average power value was within a 0.2% tolerance from that obtained with 50 periods. Convergence time was expected to increase with the increase in inflow velocity variations, which are proportional to both the amplitude and frequency of the prescribed motion. Hence, for each DOF, the simulation with the highest amplitude and frequency could have sufficed for the optimization but further investigation would be needed to confirm this. Since optimizing every simulation would not have led to any time savings, except for future studies, the compromise solution was to optimize in the corners of the amplitude-frequency domain of the prescribed motion in each DOF. A value of 15 periods after the transient period was chosen.

The RPOs for surge and pitch are shown in figures 2 and 3, respectively. Points in the contours are equidistant. Both contours have 13 points in the frequency dimension. The surge contour has 7 points in the amplitude dimension, whereas the pitch contour has 9 points. Linear interpolation was used between points. The surge, sway, heave, roll, pitch and yaw static offsets

were $x_0 = \{0\ m, 0\ m, -0.47\ m, 0.16\ deg, 3.77\ deg, 0.04\ deg\}$, respectively, and were extracted from the fully-coupled benchmarking case. The heave RPO is not shown for conciseness. The remaining DOFs were not considered since they showed negligible oscillations when compared to the three DOFs described before. These contours were produced under a wind shear profile with a below-rated wind speed of 10 m/s at hub height, aligned with the surge direction and a power-law exponent of 0.08. No turbulence was considered. The controller was enabled throughout. The turbine was modeled as being elastic. Looking at the results, the contours show two different regions. In the white zone, the values do not diverge significantly from the simulation where the turbine is fixed (origin of the contour). Increasing the frequency and amplitude together past specific values leads to an increase in average power production. This could point to power injection from the platform motion itself and the lack of responsiveness of the controller when faced with steep variations of the incoming wind speed. Although the loads were not analyzed, this was likely accompanied by an increase in their magnitude. Surging and pitching produce similar contours in the considered domains but the power production seems more sensitive to pitching. For small pitch displacements, the pitching motion can be approximated by a surge motion which can help explain why the contours are similar. The higher sensitivity to pitch likely has to do with the fact that the pitching motion induces more significant variations in the wind speed seen by the rotor as well as changes in the inflow angle. At a hub height of 135 m and frequency of 0.3 Hz, a surge and pitch motion of 3 m and 2 deg of amplitude induced a maximum axial velocity variation of 5.65 m/s and 8.88 m/s, respectively. Further analysis of the contours, the necessary resolution and interpolation type is proposed as future work.

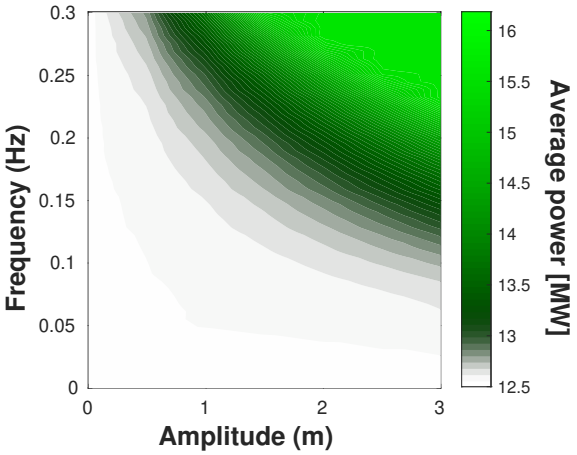

Figure 2: Surge RPOs. In the white-colored region, the average power values are close to that of the simulation where the turbine is fixed (origin). In the green region, the values are above the reference.

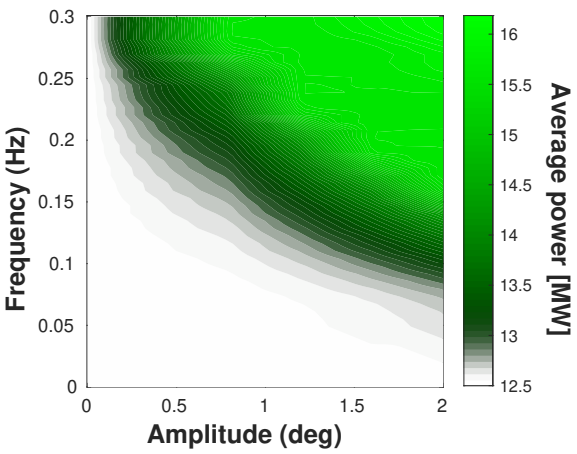

Figure 3: Pitch RPOs. See figure 2 for the color description. The value at an amplitude of 1.6 deg and 0.3 Hz was obtained by interpolating the neighboring values since the corresponding simulation crashed.

5. FOWT response spectrum - $S_{yy}(f)$

The RAO is the modulus of the complex frequency-response function of a platform DOF $H(f)$:

$$RAO(f) = |H(f)| \tag{6}$$

The RAOs are assumed to be an input from the floater designers. They can be used to estimate the response spectrum $S_{yy}(f)$ of each DOF for a sea-state spectrum $S_{xx}(f)$ [7]:

$$S_{yy}(f) = (RAO(f))^2 \cdot S_{xx}(f) \tag{7}$$

Considering very small frequency intervals around each frequency, one can estimate the equivalent amplitude spectrum as [8]:

$$A(f) \approx \sqrt{2 S_{yy}(f) \Delta f} \tag{8}$$

Δf is the inverse of the duration of the considered time series except for the transient period.

No RAO estimation was performed, so the response spectrum of the fully-coupled benchmarking case was directly used. The benchmarking case was simulated under the same conditions as the RPOs (see the previous section) but with the hydrodynamic module enabled for a full coupling. The sea-state spectrum S_{xx} was of the JONSWAP type with a significant wave height $H_s = 2.15\ m$, a peak-spectral period $T_p = 9.01\ s$ and a peak-shape parameter $\gamma = 3.3$ which are realistic values. Normally distributed waves were enabled. The simulation lasted for 10000 s, with the first 2000 s being discarded to omit the transient period. The time series were windowed with a Hamming window to limit spectral leakage with a good compromise between frequency and amplitude accuracies. The sea-state spectrum and the surge amplitude response spectrum can be seen in figures 4 and 5, respectively. It is notable that the surge spectral components are quite low for a wind speed close to rated. The largest spectral components are of the same order of magnitude as the standard deviation of the corresponding time series (that stands at 0.16), suggesting that the explanation may stem from the turbine model itself and not from the calculations. This fact was noticed and studied more in-depth in [1] and was attributed to the large inertia of this turbine. The same happens with the remaining DOFs. As a final comment, the response spectra show that the energy is largely concentrated in the same frequency bandwidth as the wave elevation, i.e., between 0.05 Hz and 0.3 Hz. Thus, only this bandwidth was considered in the AEP calculation to reduce computational cost.

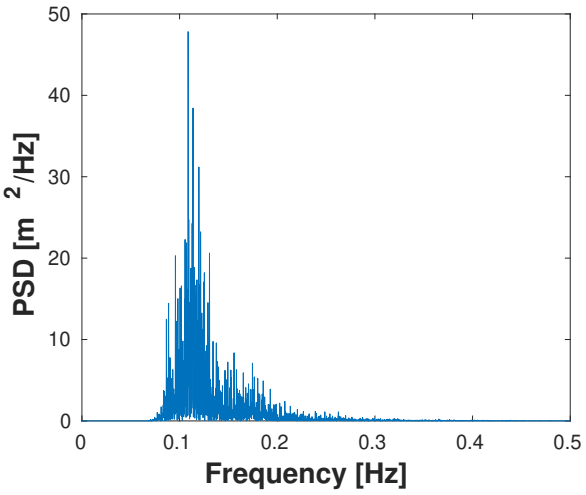

Figure 4: Sea-state spectrum $S_{xx}(f)$. The figure shows the wave elevation's power spectral density (PSD).

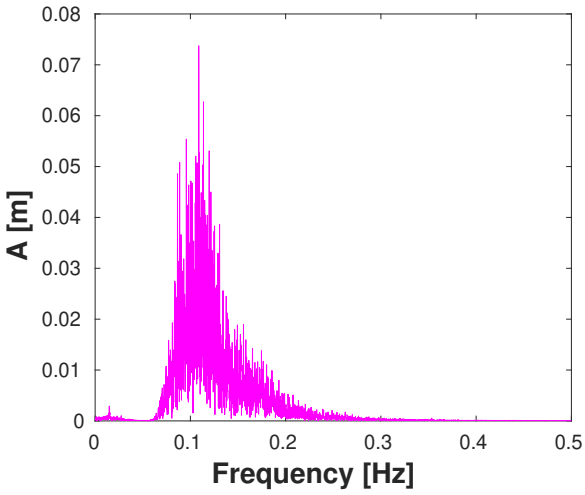

Figure 5: Surge amplitude spectrum $A(f)$. The figure shows the amplitudes estimated from the surge response spectrum.

6. Annual energy production - AEP

In order to obtain the AEP, the average power spectrum $\overline{P}(f)$ needs to be calculated. This is first done by composing the RPOs with the amplitude response spectrum $A(f)$ as follows:

$$\overline{P}(f) = RPO(A, f) \circ A(f) = RPO(A(f), f) \tag{9}$$

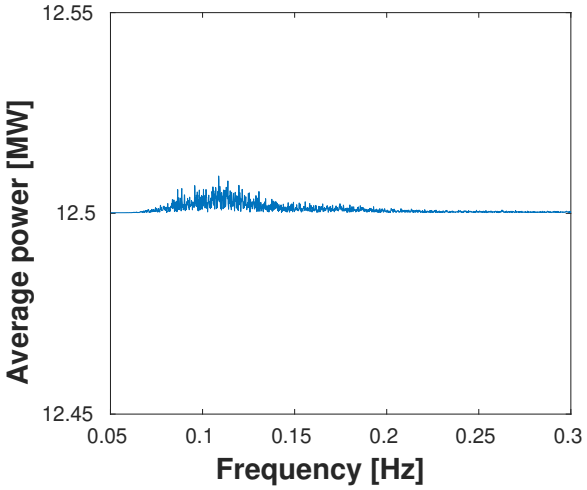

Figure 6: Surge average power spectrum. For each frequency, the figure shows the turbine's power if it were oscillating at that single frequency of the considered sea-state spectrum.

The overline in $\overline{P}(f)$ and "$\circ$" denote the averaging and composition operations, respectively.

The surge average power spectrum can now be seen in figure 6. Due to the amplitude spectrum, the variations seen in average power as a function of the frequency are tiny and the average power values are very close to those developed when the turbine is not moving. The next step is to calculate the average power $\overline{P}$ that the turbine produces under this sea-state for each DOF. For this, a simple average over the frequencies could be used. However, more weight is given to the frequency components that show the largest amplitudes, leading to, for surge:

$$\overline{P} = \overline{\overline{P}(f)} = \frac{\int_{-\infty}^{+\infty} \overline{P}(f)A(f)df}{\int_{-\infty}^{+\infty} A(f)df} \approx 12.50MW \tag{10}$$

The convolution mentioned in section 3 refers to the numerator operation of equation 10 which is similar to a convolution integral. Now, selecting only the most significant DOFs, assuming linearity and assuming that they have the same weight, the global average power $\overline{\mathbf{P}}$ is given by:

$$\overline{\mathbf{P}} = \frac{\overline{P}_{Surge} + \overline{P}_{Heave} + \overline{P}_{Pitch}}{3} \approx 12.50MW \tag{11}$$

The AEP is computed by multiplying $\overline{\mathbf{P}}$ by a one-year time scale Δt:

$$AEP = \overline{\mathbf{P}}\Delta t \tag{12}$$

The average power is enough to benchmark against the fully-coupled simulation since the time scale would have been the same. The fully-coupled simulation yields:

$$\overline{\mathbf{P_{fc}}} \approx 12.56MW \tag{13}$$

The AEP estimation shows, therefore, an error of approximately -0.47%. Although this value is low, it should be noted that the turbine was operating under almost static conditions.

Hence, it is hard to assess how the method would perform for smaller turbines with lower inertia that would undergo larger motions. In order to assess this, some more benchmarking cases were performed with larger turbine displacements. For this, fully-coupled simulations under monochromatic regular waves with a wave height of 2 m in a [0;0.1] Hz frequency range were used. The rated wind speed of 10.59 m/s was considered to maximize the resulting loads and platform motions. The duration, transient period and filtering of these time series were the same as the realistic sea-state spectrum described in the previous section. As for the prescribed motion simulations, the same due diligence described in section 4 was applied. A large bump showed up in a single roll simulation which was discarded. New offsets $x_0 = \{0\ m, 0\ m, -0.53\ m, 0.17\ deg, 4.26\ deg, 0.02\ deg\}$ according to the new wind speed were used. The considered test matrix only required ten periods to achieve average power convergence. Figure 7 shows the spectral amplitude components of the most significant DOFs. It can be seen that they are significantly higher than for the realistic sea-state considered before. The figure also shows that the maximum observed amplitudes in the time series match the spectral components at the regular wave frequency. This suggests that the regular wave frequency has the largest impact in driving the motion, as expected, and that the windowing is suitable. Under the linearity assumption implicit in equation (7), only the response at the regular wave frequency was considered. The power spectrum became then a single-valued function for each simulation. This value is plotted in figure 8 against the regular wave frequency, together with the value of the average power obtained in the corresponding fully-coupled simulation. The values are close but it is still difficult to judge if the method's assumptions are valid because the controller actions try to bring the power back to its optimal value. Therefore, the estimated values are not likely to diverge much from the fully-coupled simulations, even for large turbine motions. Turning the controller off and prescribing a rotor speed could shed some light on the matter. However, that situation would be unrealistic, making it difficult to draw conclusions for a realistic scenario with the controller enabled. Another important realization is that the average power produced when the turbine is not moving is below the rated power of 15 MW even though the turbine is operating at the rated speed. This indicates that the static offsets of the turbine drove the drop in average power from the rated power since the inclusion of waves had little impact.

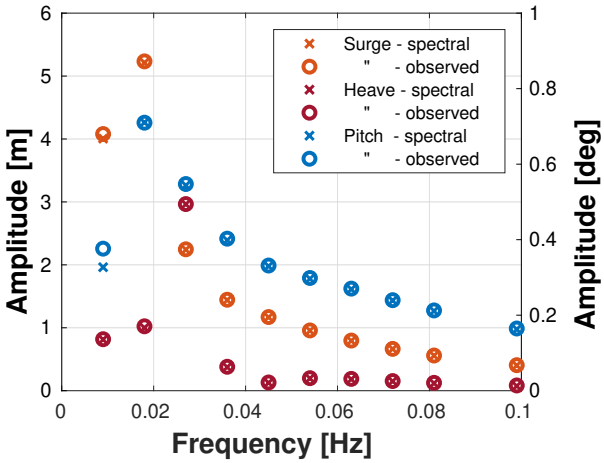

Figure 7: Spectral amplitude components and maximum observed amplitudes. The crosses indicate the spectral amplitudes. The circles indicate the largest observed amplitudes. The results for surge, heave and pitch are plotted in orange, red and blue, respectively.

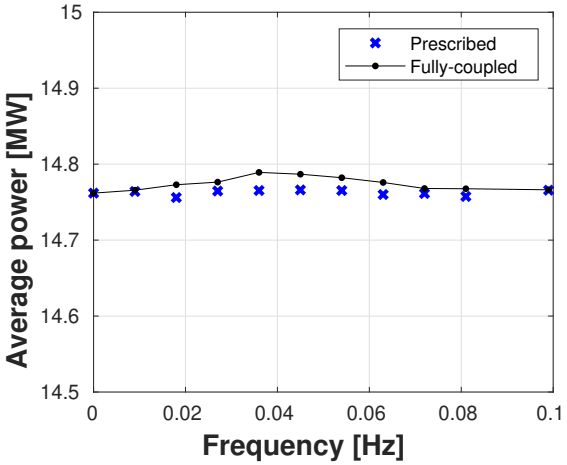

Figure 8: Average power comparison. The blue crosses match the value of the average power estimated from the prescribed motion simulations. The linked black dots match the value of the average power produced by the turbine in the fully coupled simulations.

7. Computation performance comparison

To compare the performance of this method with the traditional fully-coupled simulations, one can consider a power curve calculation with P parameters for a given site. These can be the wind speed U at hub height, the significant wave height H_s and the peak spectral period T_p, among many others. Each parameter is considered in a particular range and with a certain number of values. For simplicity, let us assume this number V is the same for each parameter. The inclusion of turbulence and stochastic sea-states requires at least six 10-minute realizations per point in the power curve. The number of fully-coupled simulations to run S'_{fc} for one set of RAOs is:

$$S'_{fc} = 6 \cdot P \cdot V \tag{14}$$

Many iterations are usually required to achieve satisfactory RAOs and more than one floater may be considered for a given site. For an average number of iterations I per floater and a number of floaters F, the total number of simulations to run S_{fc} is:

$$S_{fc} = I \cdot F \cdot S'_{fc} = 6 \cdot I \cdot F \cdot P \cdot V \tag{15}$$

On the other hand, the proposed method does not require the simulation of H_s and T_p and the simulations do not need to be repeated for subsequent iterations or floaters. However, it requires the simulation of many amplitudes and frequencies for the six DOFs. Assuming, for simplicity, that the number of amplitudes and frequencies is equal to the number of values that the other parameters can take V, the total number of prescribed motions simulations S_{pr} is:

$$S_{pr} = 6 \cdot 6 \cdot (P - 2 + 2) \cdot V = 36 \cdot P \cdot V \tag{16}$$

Let us now define the adimensional speed of a simulation as the ratio between the simulated time and the real-time elapsed during the simulation:

$$v = \frac{\Delta t_{sim}}{\Delta t_{real}} \tag{17}$$

From 186 fully-coupled simulations and 2123 prescribed motion simulations, the corresponding average speeds v_{fc} and v_{pr} in the cluster were approximately:

$$v_{fc} = 0.43 \qquad v_{pr} = 0.54$$

Only part of the aforementioned simulations was the subject of this paper but they were all used in the simulation speed calculation for more significant reliability in the result. Note that the choice of an average speed alleviates the fact that the simulation speed depends on the type of cores used and its computational load at the time of running. Thus, as expected, this calculation suggests that the fully-coupled simulations are slower than the decoupled simulations.

The last variable to factor in is the duration of the simulations. Discarding the initial transient period for simplicity, the fully-coupled simulations last ten minutes. The duration of the decoupled simulations depends on the number of prescribed periods necessary to achieve average power convergence and on the prescribed frequency. Realistic sea-states should not require frequencies outside the [0.05 0.3] Hz interval. The reported benchmarking cases required 10 and 15 periods for average power convergence in the respective RPOs domains. However, larger amplitudes and frequencies may occur for other turbines and the convergence time is expected to increase with both as the simulation becomes more unsteady. Although the relationship between convergence time and unsteadiness was not studied, let us assume some 45 periods until convergence. At an average period of 5.71 s, this gives 257.14 s until convergence. Since

this value is lower than the required duration of ten minutes to achieve statistical reliability with six realizations, a value of ten minutes must be used instead. Finally, one can compute the speed-up ratio from fully-coupled to prescribed motion simulations as the ratio of the total duration of all the fully-coupled simulations to the total duration of all the prescribed motion simulations:

$$R = \frac{S_{fc} \cdot \frac{1}{v_{fc}} \cdot \Delta t_{sim}}{S_{pr} \cdot \frac{1}{v_{pr}} \cdot \Delta t_{sim}} = \frac{6 \cdot I \cdot F \cdot P \cdot V \cdot v_{pr}}{36 \cdot P \cdot V \cdot v_{fc}} = \frac{I \cdot F \cdot v_{pr}}{6 \cdot v_{fc}} \approx \frac{I \cdot F}{5} \tag{18}$$

For the realistic case when three floaters are considered for a given site, this method outpaces the fully-coupled simulations after only two optimization iterations per floater. The high scalability of this method has to do with the fact that the RPOs are a one-time calculation for a given site and turbine. They can even be calculated in advance in the turbine design phase. Moreover, the six platform DOFs were considered in the speed-up ratio calculation but the most impactful appeared to be only surge, heave and pitch. Considering only these would effectively double the speed-up ratio. As a last optimization proposal, multiple amplitudes could even be simulated in a single simulation while ensuring a quasi-steady change in amplitude.

8. Conclusions

This paper presented and tested a method for annual energy production estimation based on frequency and time design techniques. The method combined an amplitude-frequency average power mapping, i.e., response power operators, with a floating turbine response spectrum in its most impactful DOFs to produce an average power estimate of the turbine when subjected to an arbitrary input sea-state. A realistic JONSWAP spectrum and monochromatic regular waves were used as benchmarking cases. The estimated and benchmarked average power values were close. Still, more investigation is needed since this could be a consequence of the fact that the turbine motion was minimal and the controller actions were dominant. This method proved to be highly scalable, outpacing the traditional fully-coupled simulations after the second optimization iteration when three floaters are considered for a given site and turbine.

Acknowledgments

The authors would like to thank Jason Jonkman from NREL for his responsiveness in the OpenFAST forum and all his advice on the ExtPtfm module of OpenFAST. This was key to the success of this work. We would also like to thank Mohammad Mahfouz for providing details on his turbine model. This work was carried out within the European Industrial Doctorate program STEP4WIND (H2020-MSCA-ITN-2019, grant agreement 860737).

References

[1] Mahfouz M Y, Salari M, Hernández S, Vigara F, Molins C, Trubat P, Bredmose H and Pegalar-Jurado A 2020 *Public design and FAST models of the two 15MW floater-turbine concepts* (Stuttgart: USTUTT) *Preprint*
[2] National Renewable Energy Laboratory. OpenFAST Documentation [Internet]. Boulder: National Renewable Energy Laboratory [updated 2021 November 08; cited 2022 January 10]. Available from: openfast.readthedocs.io
[3] National Renewable Energy Laboratory. IEAWindTask37 [Internet]. Golden: National Renewable Energy Laboratory [updated 2022 January 10; cited 2022 January 10]. Available from: github.com/IEAWindTask37/IEA-15-240-RWT/blob/master/OpenFAST/IEA-15-240-RWT-Monopile/ServoData/libdiscon.so
[4] Branlard E, Shields M, Anderson B, Damiani R, Wendt F, Jonkman J, Musial W 2020 *J. Phys.: Conf. Series* **1452** 1–7
[5] Asareh M A, Prowell I 2011 *Seismic Loading for FAST* (Golden, CO: NREL)
[6] Montalvão e Silva J, Maia N 2018 *Vibrações e Ruído* (Lisbon: Instituto Superior Técnico) chapter 3 pp 43-46

[7] Chakrabarti S K 1994 *Offshore Structure Modeling* (Advanced Series on Ocean Engineering vol 9) ed P L-F Liu (Singapore: World Scientific Publishing Co. Pte. Ltd.) chapter 10 pp 423-433
[8] Ochi M K 1998 *Ocean Waves* (Cambridge Ocean Technology Series vol 6) ed I Dyer, R E Taylor, J N Newman and W G Price (Singapore: World Scientific Publishing Co. Pte. Ltd.) chapter 10 pp 423-433
[9] O'Donnell D, Murphy J, and Pakrashi V 2021 *ASME Lett. in Dyn. Sys. and Cont.* **1** 021012